Materials Letters 95 (2013) 70–73

Contents lists available at SciVerse ScienceDirect

Materials Letters

journal homepage: www.elsevier.com/locate/matlet

Effect of substrate orientation on charge ordering behavior in $Sm_{0.5}Ca_{0.5}MnO_3$ epitaxial films

C.Y. Li [a], Y.Q. Wang [a,*], R.S. Cai [a], Y.Z. Chen [b], J.R. Sun [b]

[a] The Cultivation Base for State Key Laboratory, Qingdao University, No. 308 Ningxia Road, Qingdao 266071, PR China
[b] State Key Laboratory of Magnetism and Beijing National Laboratory for Condensed Matter Physics, Institute of Physics, Chinese Academy of Sciences, Beijing 100080, PR China

ARTICLE INFO

Article history:
Received 27 November 2012
Accepted 26 December 2012
Available online 3 January 2013

Keywords:
Thin film
Epitaxial growth
Magnetic materials
Electron microscopy

ABSTRACT

The effect of anisotropic strain induced by $SrTiO_3$ (STO) substrate with different orientations on charge ordering (CO) behavior in epitaxial $Sm_{0.5}Ca_{0.5}MnO_3$ (SCMO) films was investigated using cross-sectional transmission electron microscopy at 103 K. Incommensurate modulated structure caused by CO transition was observed in the SCMO film grown on a [101]-oriented STO substrate while none were found for SCMO film grown on a [100]-oriented STO substrate. This distinctive orientation-dependent CO transition is correlated with anisotropic strain in the films induced by lattice mismatch, confirming the previous results for growth on different substrates.

© 2013 Elsevier B.V. All rights reserved.

1. Introduction

Perovskite manganites have received great attention because of their rich physical properties and potential applications for various functional devices in the field of high-density magnetic heads and sensors [1]. Besides the colossal magnetoresistance effect, charge ordering (CO) is probably one of the most fascinating properties of the perovskite manganites [2]. Compared to bulk manganite materials, CO behaviors of thin films are quite different. It has been demonstrated that these differences are strongly dependent on the strain state in the films [3,4].

In order to elucidate the influence of anisotropic strain on the properties of manganite films, extensive research has been carried out on different manganite systems [5–11]. It has been shown that the strain in the films can be controlled by film thickness, substrate type and substrate orientation. Chen et al. [5,6] and Ding et al. [7] reported the strain effect induced by changing film thickness on CO transition. Perovskite manganite films grown on different substrates with the same orientation, for example, $Pr_{0.5}Ca_{0.5}MnO_3$ (PCMO) [8], $Nd_{0.5}Ca_{0.5}MnO_3$ (NCMO) [9] and $Sm_{0.5}Ca_{0.5}MnO_3$ (SCMO) [10] grown on (100) $SrTiO_3$ (STO) and $LaAlO_3$ (LAO), exhibit different CO behaviors due to distinct film strain states related to different substrates. Chen et al. [11] studied the physical properties of SCMO films grown on STO with different orientations. However, confusion still exists about the correlation between the stability of CO state and the anisotropic strain in manganite films, *i.e.*, in what strain states do the CO transitions take place. In addition, little direct experimental evidence, such as cross-sectional transmission electron microscopy (TEM) study, is available concerning the effects of strain induced by the substrates with different orientations on the CO behaviors in SCMO films.

In this paper, we report a detailed microstructure investigation of SCMO films epitaxially grown on (100) and (101) STO. Selected-area electron diffraction (SAED) and high-resolution transmission electron microscopy (HRTEM) were used to investigate the effect of substrate-induced strain on CO behaviors in SCMO films.

2. Experimental

A ~150-nm-thick film of SCMO was epitaxially grown on (100) and (101) STO substrates using pulsed laser deposition technique. During the deposition, the temperature was kept at ~700 °C and the oxygen pressure at ~60 Pa. X-ray diffraction analysis showed that both films possess an orthorhombic crystal structure ($a \approx b \approx c/\sqrt{2}$) with a space group of *Pnma*. Specimens for TEM examinations were prepared in a cross-sectional orientation using mechanical polishing and ion thinning techniques. SAED, HRTEM and energy dispersive X-ray spectroscopy (EDS) examinations were carried out using a JEOL JEM 2100F transmission electron microscope operating at 200 kV. The temperature was controlled by a Gatan smartset cold stage controller (636.MA). TEM studies were carried out at room temperature and at 103 K.

3. Results and discussion

Fig. 1(a) and (b) shows bright field (BF) TEM images of cross-sectional SCMO/(100)STO and SCMO/(101)STO samples, respectively. These images are taken under a two-beam condition with $\mathbf{g}=10\bar{1}$

* Corresponding author. Tel.: +86 532 83780318.
E-mail address: yqwang@qdu.edu.cn (Y.Q. Wang).

0167-577X/$ - see front matter © 2013 Elsevier B.V. All rights reserved.
http://dx.doi.org/10.1016/j.matlet.2012.12.097

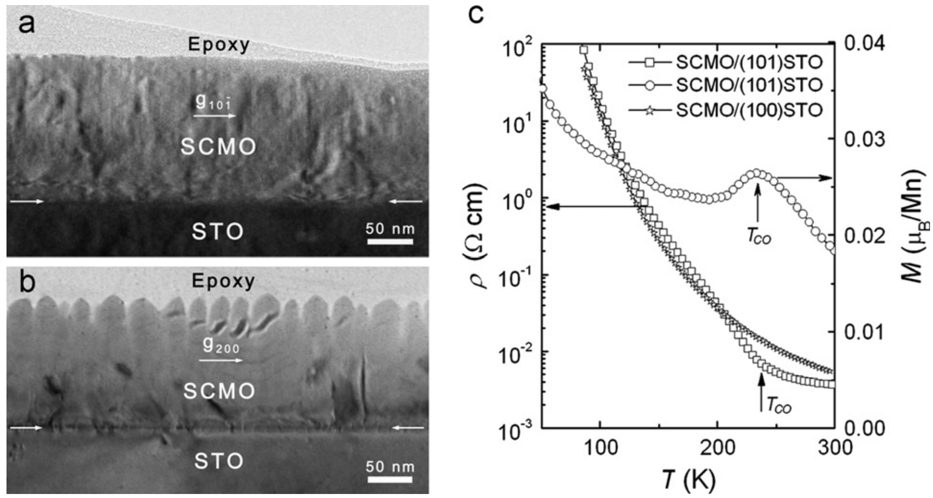

Fig. 1. Cross-sectional BF image of SCMO/(100)STO (a) and SCMO/(101)STO (b); (c) ρ–T and M–T curves for SCMO/(100)STO and SCMO/(101)STO.

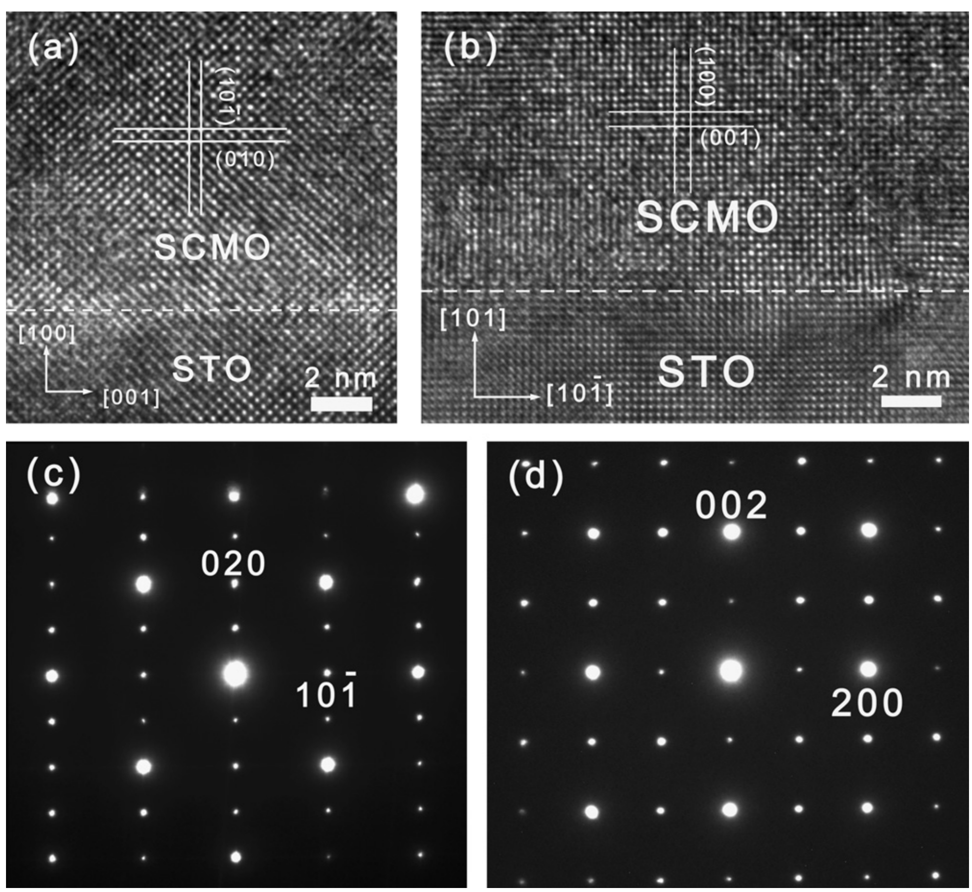

Fig. 2. Room temperature HRTEM images of SCMO/(100)STO (a) and SCMO/(101)STO (b); SAED patterns from the sample of SCMO/(100)STO (c) and SCMO/(101)STO (d).

and $\boldsymbol{g}=200$, correspondingly. The thicknesses of both films are measured to be $\sim$150 nm. It can be seen from Fig. 1(a) and (b) that the free surface is flat for SCMO/(100)STO film, while it exhibits a column-like morphology for SCMO/(101)STO film. EDS measurements indicated that both films have a chemical formula of $Sm_{0.5}Ca_{0.5}MnO_3$ within the measurement accuracy. Fig. 1(c) shows the temperature-dependent resistivity (ρ–T) and magnetization (M–T) of SCMO/(100)STO and SCMO/(101)STO films under 2 T. For SCMO/(101)STO films, a CO transition can be found at $\sim$235 K, characterized by an obvious resistivity jump and a concomitant magnetization peak. However, for SCMO/(100)STO films, the ρ–T curve is smooth, demonstrating no evident CO transition.

Fig. 2(a) and (b) shows HRTEM images of the SCMO/(100)STO and SCMO/(101)STO films, respectively, recorded at room temperature while Fig. 2(c) and (d) shows the corresponding SAED patterns. No extra diffraction spots other than the fundamental Bragg reflections in SAED patterns or modulations in HRTEM images can be observed, indicating that both films are in the charge-and-orbital-disordered state at room temperature. The SCMO/(100)STO film has a crystallographic relationship of $(10\bar{1})$SCMO$\|$(001)STO and

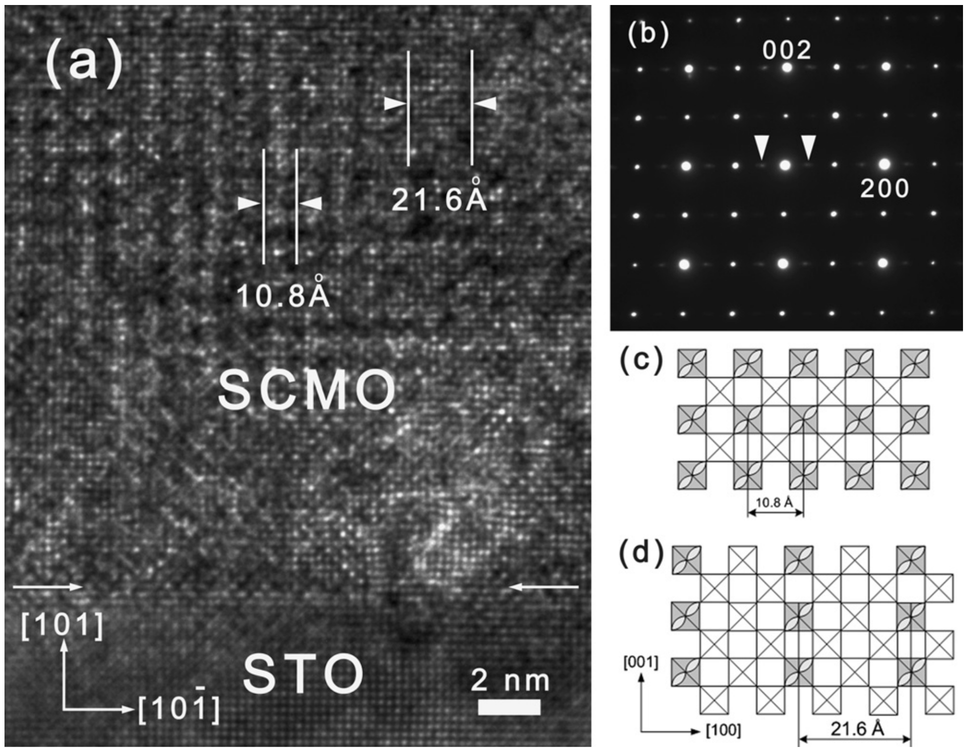

Fig. 3. HRTEM images (a) and SAED patterns (b) of SCMO/(10 1)STO films at 103 K; (c) and (d) schematic models for the incommensurate modulated structures in the SCMO/(101)STO films. ▨ and ⊠ represent Mn^{3+} and Mn^{4+}, respectively.

[101]SCMO‖[010]STO with the substrate while that for SCMO/(101)STO film is (100)SCMO‖(10$\bar{1}$)STO and [010]SCMO‖[010]STO. For the SCMO/(100)STO films, they are [010] oriented as shown in Fig. 2(a) and (c), while the SCMO/(101)STO films are [001] oriented as shown in Fig. 2(b) and (d). Usually, the film prefers to choose an orientation with a lower lattice mismatch between the film and the substrate during the film deposition. In our experiment, for the SCMO/(100)STO film, the lattice mismatch (2.07%) between (10$\bar{1}$) plane of SCMO and (001) plane of STO is lower than that between (010) plane of SCMO and (001) plane of STO (2.82%). Therefore, it is energetically more favorable for the SCMO film to be [010]-oriented when deposited on (100) STO.

For the films grown on (100) STO, no modulation structure is found (not shown here) whereas obvious modulated structures were detected for SCMO/(101)STO films recorded at 103 K. Fig. 3(a) is a typical HRTEM image of the SCMO/(101)STO film recorded at 103 K. Clear stripes can be observed in the image, which indicates the appearance of the CO state. The modulated stripes have formed along the [100] direction of the film. In most regions the periodicity of the modulation is ~10.8 Å, while in some local regions the periodicity becomes ~21.6 Å, exhibiting a characteristic of incommensurate modulations. Fig. 3(b) is a [010] zone-axis SAED pattern taken from SCMO/(101)STO film at 103 K. Superlattice spots along [100] direction are visible, implying that a clear CO transition takes place in the film, which is consistent with the HRTEM results obtained at 103 K. It can be seen from Fig. 3(b) that the superlattice spots are not located exactly in the middle position between the transmitted and diffracted spots. The modulation periodicity is determined to be 13.5 Å from the SAED pattern, which results from the incommensurate modulations with various periodicities in different regions of the film. Based on the SAED and HRTEM observations, structural models (after Wang et al. [2]) are proposed, as schematically shown in Fig. 3(c) and (d). Two different types of modulated structures are proposed along the [100] direction of the film, exhibiting an ordered arrangement of Mn^{3+} and Mn^{4+} in the film due to the strain effects. The strains in some local regions of the film could be released due to the formation of defects and then the strain in the film becomes inhomogeneous. So the ratios of Mn^{3+} to Mn^{4+} change to 1:3 from 1:1 in the local regions as shown in Fig. 3(c) and (d).

For SCMO/(100)STO film, the in-plane parameters for (10$\bar{1}$) plane of SCMO and (001) plane of STO are measured to be 3.824 Å and 3.905 Å, respectively. In this case, the calculated lattice mismatch is positive (+2.07%), which induces a compressive strain along the [10$\bar{1}$] direction and a tensile strain along the [010] direction. Thus the *a* and *c* parameters decrease and the *b* parameter increases in order to keep the same volume of the unit cell. This distortion creates a structural deformation against the Jahn–Teller (J–T) distortion and, consequently, no CO transition occurs in SCMO/(100)STO film. However, for SCMO/(101)STO film, the lattice spacings for (101) plane of SCMO and (100) plane of STO are measured to be 3.945 Å and 3.901 Å respectively. Under this condition, the negative lattice mismatch (−1.12%) induces a tensile strain along the [101] direction and a compressive strain along the [010] direction. As a result, for the SCMO/(101) STO film, the *a* and *c* parameters increase and the *b* parameter decreases. This distortion provokes a structural deformation which reinforces the J–T distortion and thus stabilizes the CO state. It confirms the previous results that distinctive CO transition can be observed in PCMO [8] and NCMO [9] films grown on (100) STO which are subjected to a tensile strain along [101] direction and a compressive strain along [010] direction. However, for SCMO [10] films grown on (100) STO, the strain states agree with those of the SCMO film on (100) STO in our experiment and no CO transition occurs. Therefore, a correlation can be found between the CO transition and the strain states of the perovskite manganite films. If the substrate-induced strain can provoke a structural deformation which favors the J–T distortion, a clear CO transition would appear. However, if the deformation provoked by the substrate-induced strain is opposite to the J–T distortion, no CO transition would happen in the films.

4. Conclusions

In conclusion, the effects of strain induced by STO substrates with different orientations on CO behavior in SCMO epitaxial films were investigated. It has been shown that incommensurate modulations are observed in SCMO films grown on (101) STO, but not on (100) STO at 103 K. A correlation between the CO transition and the strain state of the perovskite manganite films is established.

Acknowledgments

The authors would like to thank the financial support from the National Natural Science Foundation of China (Grant nos. 10974105 and 50832007), the Natural Science Foundation for Outstanding Young Scientists in Shandong Province (Grant no. JQ201002), the Project of Introducing Talents to Support Thousand Talents Programs (Grant no. P201101032), the Program of Science and Technology in Qingdao City (Grant no. 11-2-4-23-hz), and the Scientific Research Starting Foundation for the Introduced Talents at Qingdao University (Grant no. 06300701). Y.Q. Wang would also like to thank the financial support from the Taishan Outstanding Overseas Scholar Program in Shandong Province.

References

[1] Jin KX, Chen CL, Wang SL, Wang YL, Wang YC. J Appl Phys 2004;96 1537/1-3.
[2] Wang YQ, Duan XF, Wang ZH, Shen BG. Appl Phys Lett 2001;78:2157–9.
[3] Barnabé A, Hervieu M, Martin C, Maignan A, Raveau B. J Mater Chem 1998;8:1405–11.
[4] Okuyama D, Nakamura M, Wakabayashi Y, et al. Appl Phys Lett 2009;95:3545–51.
[5] Chen YZ, Sun JR, Liang S, Lv WM, Shen BG, Wu WB. J Appl Phys 2008;103 096105/1-3.
[6] Chen YZ, Sun JR, Liang S, Lu WM, Shen BG. J Appl Phys 2008;104 113913/1-4.
[7] Ding YH, Wang YQ, Cai RS, Chen YZ, Sun JR. Appl Phys Lett 2011;99 191914/1-3.
[8] Prellier W, Haghiri-Gosnet AM, Mercey B, et al. Appl Phys Lett 2000;77:1023–5.
[9] Rauwel BE, Prellier W, Mercey B, et al. J Phys: Condens Matter 2002;14:3951–8.
[10] Rauwel E, Prellier W, Mercey B, De BS, Chouteau G. J Appl Phys 2005;98 093903/1-6.
[11] Chen YZ, Sun JR, Zhao JL, et al. J Phys: Condens Matter 2009;21 442001/1-4.